A Rock Physics and Attenuation Analysis of a Well from the Gulf of Mexico

Gary. Mavko, Stanford University, Jack Dvorkin, Stanford University and Rock Solid Images, Joel Walls, Rock Solid Images*

Abstract

The well selected for the application of our attenuation theory and extraction of attenuation attributes from seismic data is the Texaco well (API 177104132700) in Block 313 of Eugene Island in the Gulf of Mexico (Well 2700). The rock physics diagnostics indicates that the rock can be described by the uncemented (soft-sand) model. This model is used to predict the S-wave velocity that was missing in the original well data. The P- and S-wave inverse quality factors are computed according to our theoretical model. The ratio of these inverse quality factors (P-to-S) is small (on the order of one) in wet rock and large in the gas zone. The seismically-measured attenuation ratio may serve, therefore, as an indicator of hydrocarbons. The synthetic seismic traces computed using the well data and the ray-tracer with attenuation, specifically developed for this project, indicate that attenuation affects the seismic response and, therefore, can be extracted from real seismic data, including the P-to-P and P-to-S reflection amplitude.

Rock Physics Diagnostics – Model for Velocity

The gas saturation in the well was calculated from the resistivity curve while the clay content was estimated by linearly scaling the gamma-ray curve between its minimum and maximum values. It was assumed that the formation water has the bulk modulus 2.85 GPa and density 1.01 g/cc while the gas has the bulk modulus 0.14 GPa and density 0.26 g/cc. The total porosity was calculated from the bulk density by assuming that the density tool samples the virgin formation with gas saturation as calculated from resistivity.

The measured impedance and P-wave velocity are compared to the curves due to the uncemented (soft-sand) model. The proximity of the data and model (Figure 1) indicates that this model is appropriate for the well under examination. This model was then use to predict the S-wave velocity (absent in the measured data) from the P-wave velocity.

The in-situ impedance is plotted versus the total porosity and Poisson's ratio (PR) in Figure 2 where the data are color-coded by gamma-ray and by water saturation. Similar cross-plots are shown in Figure 3 but for wet conditions where the elastic properties and density were calculated using the P-wave-only fluid substitution. The soft-sand model curves for water-saturated rock are superimposed upon the wet-condition data to further emphasize the relevance of this model. The curves are produced for varying porosity and each for fixed clay content. The latter variable changes from one to zero with step 0.2. These model curves fully encompass the well log data.

Attenuation Modeling

Theoretical development of rock phyics models for P-wave attenuation are presented in two papers by Dvorkin, et al, 2003. Theory behind the S-wave attenuation computation is presented in Mavko, et al, 2005. We have used these models to compute the attenuation curves on well 2700. The results of P- and S-wave attenuation modeling indicate that the P-wave inverse quality factor (Q_p^{-1}) is only significant in the gas reservoir and small elsewhere (Figure 4 and 5). The inverse S-wave quality factor (Q_s^{-1}) is small everywhere in the interval and close to Q_p^{-1} as calculated in wet rock.

Figure 6 displays the ratio of the P-to-S inverse quality factors (Q_p^{-1}/Q_s^{-1}) plotted versus the P-to-S-wave velocity ratio (V_p/V_s) and color-coded by water saturation (S_w). This cross-plot is for the in-situ conditions.

The low V_p/V_s is typical of gas sand where Q_p^{-1}/Q_s^{-1} is coincidentally large. Therefore, these attributes as well as their hybrids, when extracted from seismic data, may serve as hydrocarbon indicators.

Notice that for the wet low-gamma-ray sand in the bottom part of the well Q_p^{-1}/Q_s^{-1} is small although the V_p/V_s (and PR) contrast between this sand and surrounding shale is negative (but not as strong as in the gas sand). This negative contrast may still produce an AVO anomaly that can be mistakenly attributed to a gas reservoir (Figure 7). Under such circumstances, the attenuation ratio (Q_p^{-1}/Q_s^{-1}) may serve as a unique hydrocarbon indicator.

Raytracer

A synthetic-seismic raytracer has been created specifically for this project to estimate the effects of the elastic rock properties and attenuation on the seismic amplitude and attributes. The raytracer produces P-to-P as well as P-to-S (converted shear) gathers. The algorithm takes into account both P- and S-wave attenuation by means of a Q-filter.

Synthetic Modeling

The results of synthetic seismic modeling with and without taking attenuation into account are displayed in

Figure 8 and 9. The P-to-P amplitude (Figure 8) is noticeably affected by the attenuation for both normal incident and offset traces. This result implies that the P-wave attenuation (Q_p^{-1}) can be extracted from real seismic data.

The converted-wave (P-to-S) traces in Figure 9 reflect the fact that the S-wave attenuation is small – the synthetic amplitude computed with attenuation is not very different from that computed without attenuation. To test whether Q_s^{-1} indeed affects the converted-wave amplitude in this synthetic modeling, we compute a far-offset trace with Q_s^{-1} ten time that predicted by our rock physics modeling (Figure 9, separate frame at the bottom). The apparent effect of attenuation on the amplitude is large which means that the S-wave attenuation (Q_s^{-1}) can be extracted from real seismic converted-wave data.

Conclusion

A new rock physics model allows for estimating P- and S-wave attenuation from standard well log data. It implied that while the P-wave attenuation is noticeably affected by the presence of hydrocarbons, the S-wave attenuation is not. The model predicts that the ratio of these attenuation values can be used as a hydrocarbon indicator.

A large potential of this model is that it allows for consistent forward modeling of attenuation depending on the properties and conditions in the subsurface to supplement and extend the existing real data. Such rock-physics-based "what-if" forward modeling is a powerful tool of seismic interpretation and has been extensively used with the elastic properties. Our new theoretical development helps extend this approach into the inelastic domain.

Of course, attenuation can be used in exploration and development only if it can be extracted from real seismic data. To test whether such extraction is viable, we create synthetic seismic traces for P-to-P and P-to-S amplitude using our rock physics predictions. In this synthetic modeling we use a new raytracer tool designed specifically for this task. The results prove that the amplitude is indeed affected by attenuation and, therefore, by inference, we conclude that the seismic P- and S-wave attenuation can be measured in the field and eventually used for the purpose of rock diagnostics.

Future development will include close work with real seismic and well log data to further calibrate and validate the proposed methods of reservoir characterization as well as to chart the areas of their applicability.

Acknowledgements

The work was supported by Rock Solid Images and the US Dept. of Energy (under contract DE-FC26-04NT42243).

References

Dvorkin, J., G. Mavko, J. Walls, M.T. Taner, N. Derzhi, 2003; Attenuation at Patchy Saturation – A Model, Proceedings of Annual EAGE Convention, Stavanger Norway, June 2-5.

Dvorkin, J., G. Mavko, and J. Walls, 2003; Seismic wave attenuation at full water saturation, Proceedings SEG Intl. Exposition and 73rd Annual Meeting, Dallas, TX, Oct 26-31.

G. Mavko, Dvorkin, J., and J. Walls, 2005; A Theoretical Estimate of S-Wave Attenuation in Sediment, Proceedings SEG Intl. Exposition and 75th Annual Meeting, Houston, TX, 6-11 November.

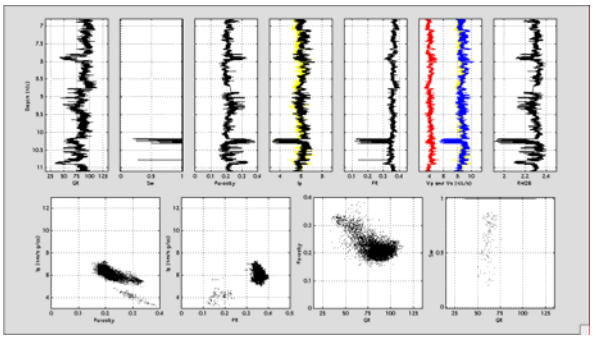

Figure 1. Log data display for Well 2700 under examination. Top, from left to right -- gamma-ray; water saturation; total porosity; P-wave impedance; Poisson's ratio (predicted); P- and S-wave (predicted) velocity; and bulk density. Bottom, form left to right – impedance versus porosity; impedance versus Poisson's ratio; porosity versus gamma-ray; and water saturation versus gamma-ray. The yellow curves superimposed upon the data in the impedance and velocity frames in the top row are calculated from the soft-sand model using the porosity and clay as well as the pore-fluid properties as inputs.

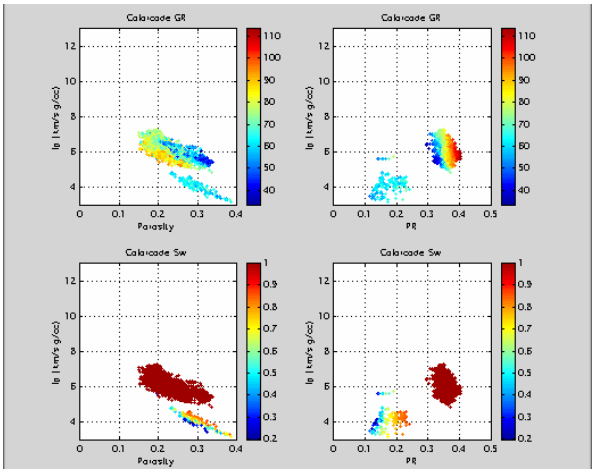

Figure 2. Impedance versus porosity (left) and versus Poisson's ratio (right). The data in the top row are color-coded by GR while that in the bottom row are color-coded by water saturation. In situ data.

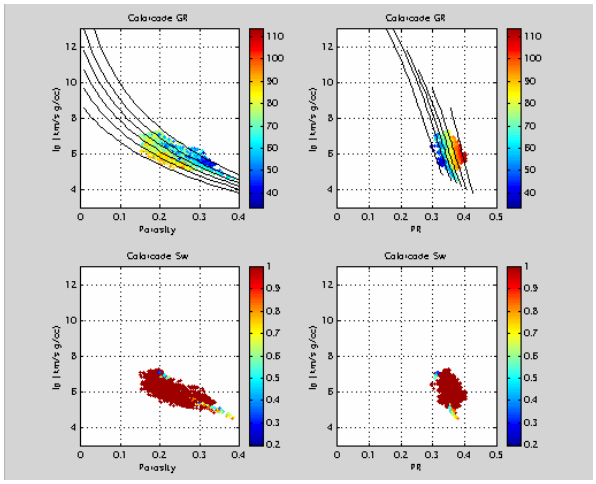

Figure 3. Same as Figure 2 but for wet conditions. The model curves in the top row are from the soft-sand model for clay content varying from one (top curve in the impedance-porosity display and left-most curve in the impedance-PR display) to zero with step 0.2.

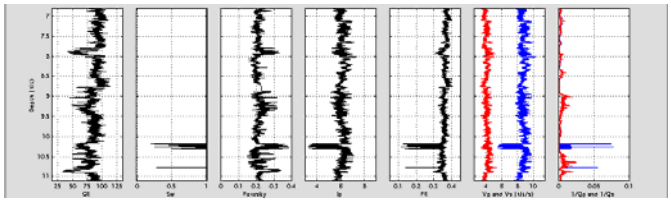

Figure 4. Well log display with the inverse quality factor shown in the last frame (P in blue and S in red).

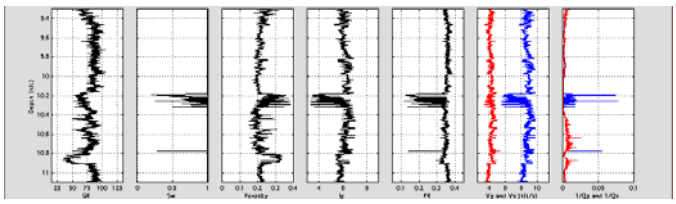

Figure 5. Same as Figure 4, zoomed on the bottom part of the well.

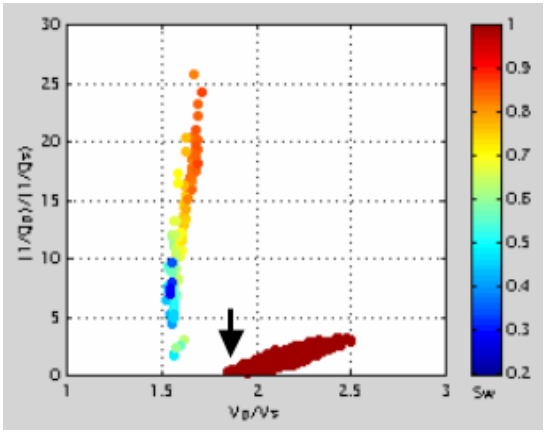

Figure 6. Inverse quality factor ratio versus velocity ratio from Figure 4 color-coded by water saturation. The arrow point to the data for the two wet sand intervals located just above 8 and 11 kft (see GR track in Figure 4).

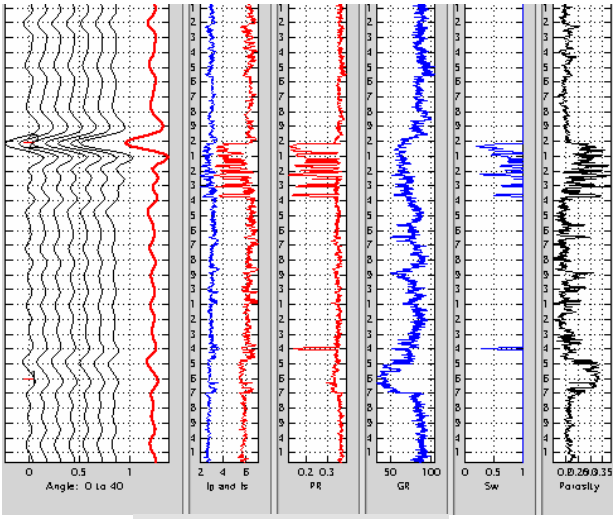

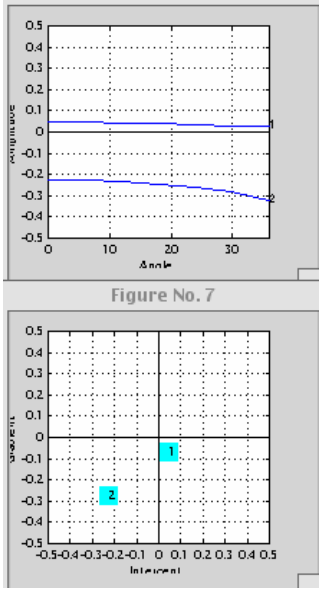

Figure 7. Synthetic seismic traces (40 Hz) in the bottom part of the well showing that the wet sand (pick "1" on the gather) may exhibit a negative gradient although not as strong as gas sand (pick "2" on the gather). From left to right – gather (black) and stack (red); P- and S-wave impedance; Poisson's ratio; GR; water saturation; and porosity. The AVO curves and gradient-versus-intercept plots are at the picks shown in numbers on the gather display.

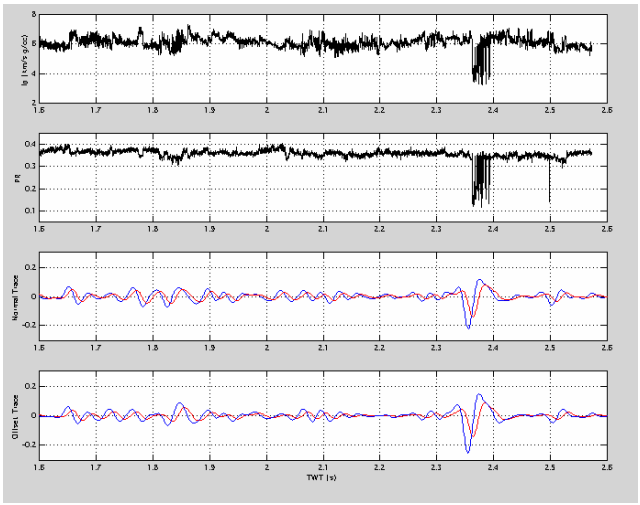

Figure 8. Synthetic raytracer modeling at 40 Hz. P-to-P reflection. From top to bottom – impedance; PR; normal-incidence trace; and offset trace versus P-wave TWT. The blue traces in the bottom two frames are calculated without attenuation while the red traces are calculated with taking the P-wave attenuation into account.

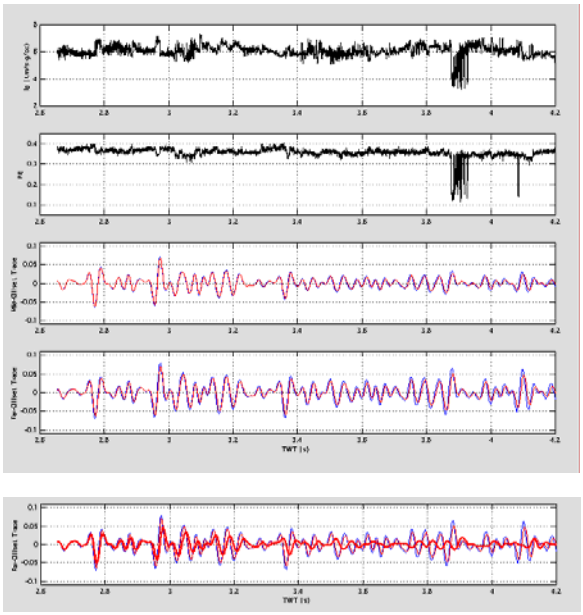

Figure 9. Same as Figure 8 but for P-to-S reflections. The red traces are calculated with taking the P- and S-wave attenuation into account. The separate frame at the bottom also displays the far-offset trace calculated for the S-wave attenuation ten times as that predicted by the rock physics model (bold red trace).